International Journal of Innovation and Applied Studies
ISSN 2028-9324 Vol. 8 No. 3 Sep. 2014, pp. 1204-1212

http://www.ijias.issr-journals.org/

Removing Gradient and Ballistocardiographic Artifacts from EEG using FMRIB Toolox

Rabeya Ferdousy and Prof. Dr. Subrata Kumar Aditya

Department of Applied Physics, Electronics and Communication Engineering,
University of Dhaka,
Dhaka, Bangladesh

ABSTRACT: Real-time recording of the electroencephalogram (EEG) and functional magnetic resonance imaging (fMRI) may reveal the brain's activity at high temporal and spatial resolution. However, the EEG recorded during fMRI scanning is corrupted by large repetitive artifacts, called Gradient artifacts which are generated by the switched MR gradients. In addition, Ballistocardiographic artifacts (BCG) are overlaid on the EEG resulting from heart beat related body movements and blood flow changes. This thesis presents generic methods to remove fMRI environment-related artifacts from EEG data with the minimization of residual artifacts. Firstly, methods for removing gradient and BCG artifacts have been presented in this thesis which is based on capturing temporal variations in the artifacts by carrying out temporal principal component analysis (PCA) and recognition of a set of basis functions which describe the temporal variations in the artifacts. FASTR (fMRI Artifact Slice Template Removal) algorithm is used here for subtracting gradient artifacts in which a unique artifact template is generated for each slice as the local moving average plus a linear combination of basis functions that describe the variation of residuals. The basis functions are derived by performing temporal principal component analysis (PCA) on the artifact residuals and selecting the dominant components to serve as a basis set. QRS complexes are identified for the purpose of pulse artifact removal. These methods are implemented as an FMRIB toolbox in EEGLAB. The algorithms employed here give satisfactory results by removing all the artifacts. This artifact reducing analysis offers possibilities for improved neurological research and clinical neurosurgical applications.

KEYWORDS: Electroencephalogram (EEG), Gradient Artifacts, Ballistocardiographic Artifacts, Principle Component Analysis (PCA), Optimal Basis Set (OBS)**,** Magnetic Resonance Imaging (MRI), Functional Magnetic Resonance Imaging (fMRI).

1 INTRODUCTION

Combined EEG/fMRI recording has been used to localize the generators of EEG events and to identify subject state in cognitive studies and is of increasing interest [1]. EEG recordings obtained inside the MR environments suffer from various kinds of artifact. There are two physical principles which underlie the generation of these artifacts. First, if the magnetic flux through a loop changes, an electromotive force (emf) is induced in the loop (Faraday's induction law). Second, there is a blood flow effect, whereby the movement of blood (a conductor) normal to a magnetic field leads to induced potentials. These principles result in two prominent types of artifacts. First, gradient artifacts are caused by the switching of magnetic gradients during FMRI. Second, ballistocardiographic (BCG) artifacts related to cardiac activities further contaminate the EEG data.

The switching of magnetic gradients is necessary for MRI image acquisition; and the related EEG signal distortions cannot be avoided by any shielding. Interleaved designs, where EEG recordings are analyzed during the "silent" interval between MR scanning, have been used, but they do not solve the principle problem and restrict the efficiency of the experiment. The two types of imaging artifact that can be distinguished are the gradient artifact (GA), which causes a massive distortion of the EEG, and radio frequency (RF) artifact. Because the latter has a much higher frequency than the EEG signal, it can be effectively suppressed by analog low pass filtering. Analog low pass filtering is mandatory anyway to avoid EEG amplifier saturation and aliasing problems. Accordingly, the GA represents the major source of MR imaging artifact. The GA is a

Corresponding Author: Rabeya Ferdousy

technical or exogenous artifact that reflects the imaging slice acquisition. Its major contribution is a very steep rising, transient signal with gradients that can be in the order of millivolts per millisecond. The GA completely dominates the EEG recording during MR image acquisition periods. Unlike the RF, the GA distorts the EEG spectrum over a broad frequency, including the frequency range of interest (< 100 Hz), and therefore cannot be fully accounted for by filtering. In fact, for many purposes, the GA is one of the two major artifacts that need to be dealt with statistically [2].

Different approaches have been proposed to remove gradient artifacts from biological signals collected during MRI scanning. Hoffmann proposed a frequency domain method, where the amplitude and phase of the data were set to zero at frequencies matching an artifact power spectrum template [3]. However, this approach suffers from the typical Fringing_ effect common to such frequency domain filters [4]. The most used method is average artifact subtraction [4, 5]. This utilizes the repetitiveness of the artifact to form an average artifact template, which is then subtracted from the EEG data. The efficacy of this approach has been demonstrated in the literature [4, 5, 6], though a number of quality and practicality issues still remain. Firstly, some residual artifacts remain on some channels. Allen proposed the use of adaptive noise cancellation (ANC) to remove these residuals; however, this approach does not remove all residual artifacts [5]. Secondly, in order to minimize the residuals, a high sampling frequency is needed [7].

In this paper, a method for the removal of gradient artifacts; FMRI artifact slice template removal (FASTR) is presented. In FASTR, a unique artifact template for each slice artifact in each EEG channel is constructed and then subtracted. Each slice template is constructed as the local moving average plus a linear combination of basis functions that describe the variation of residuals. The basis functions are derived by performing temporal principal component analysis (PCA) on the artifact residuals and selecting the dominant components to serve as a basis set. This technique is superior and applicable at a sampling rate as low as 2048 Hz.

Unlike the GA, which occurs only during slice acquisition periods, the ballistocardiogram (BCG) is always present in the scanner's magnetic field. The BCG contributes to the low frequency portion of the EEG signal (< 15 Hz). A concurrent recording of the EEG with the electrocardiogram (ECG) reveals that the periodic distortion present in most EEG channels is related to the cardiac cycle. While the exact origin of the BCG is not known yet, it is likely that the pulsatile flow of blood associated with the cardiac cycle induces a rocking, nodding head motion. Another source of influence could be that EEG electrodes (or cables) over, or adjacent to, pulsatile blood vessels are in steady motion. And finally, according to the Hall effect, the acceleration of blood, which is electrically conductive, could be a source of current induction that is registered in the EEG [8].

Several approaches have been proposed to remove the BCG artifact. Adaptive filtering has been proposed by Bonmassar : a piezoelectric sensor was used to generate a reference BCG signal, which was then used to filter out BCG contributions from the EEG [9]. This method is computationally expensive, requires the use of an extra sensor and assumes that no EEG correlated information is present in the sensor signal. Spatial PCA and independent component analysis (ICA) filters have also been proposed [4]. One problem with these approaches is that they necessitate the presence of a large number of sensors. Also, the identification of artifact components can be subjective and is usually done manually. Most importantly, spatial filters assume that all the sensors are contaminated by common sources, which is not the case. The BCG artifact derives from sources that are rotating/moving, which contaminate different sensors at different points during the cardiac cycle with different effects. The most commonly used method for removing the BCG artifact is the average artifact subtraction (AAS) [1], in which a moving average artifact template is computed from successive artifact occurrences, then subtracted from the data. This assumes that the BCG artifact is a slowly changing signal that can be accurately captured by a moving average. This can result in residual artifacts in the data [7].

In this study, a method where a basis set is constructed by performing temporal PCA on each EEG channel data has been exploited. The basis set is then fitted to, and subtracted from, each artifact occurrence. This approach has the advantage of not assuming any temporal relation between the different occurrences of the BCG artifact in a given EEG channel. Rather, the assumption is that over a sufficient period of EEG recording from any single EEG channel, the different BCG artifact occurrences in that channel are all sampled from a constant pool of possible shapes, amplitudes and scales. The principal components of all the occurrences can then describe most of the variations of the BCG artifact in that channel.

2 METHODS

2.1 THE GRADIENT ARTIFACT REMOVAL

During MR imaging, the magnetic field inside the MRI scanner continuously changes as a result of the switching of the magnetic field gradients [7]. The gradients change according to the imaging sequence being used. In an echo planar imaging

(EPI) sequence typically used in FMRI, gradient switching is repeated each time a new slice is collected, resulting in artifacts that repeat with the collection of each new FMRI slice. The amplitude of such artifact can be 100 times greater than the EEG signal and its frequency content overlaps that of the EEG, thus gradient artifacts cannot be simply filtered out. The artifact shape and amplitude varies from one EEG channel to another depending on the location of the electrodes and the wire connections [3, 10, 11].

FASTR (fMRI Artifact Slice Template Removal) algorithm

In this paper, an algorithm named 'FASTR' is presented which is used to remove the gradient artifact. FMRI artifact slice template removal, FASTR is based on constructing a unique template for each artifact segment, in each channel, generated during the acquisition of a single FMRI slice. The algorithm comprises four steps. First, the signal is interpolated (up-sampled) and the slice-timing triggers are adjusted to optimize the alignment. Second, a local artifact template subtraction is performed, in which a moving average artifact template is constructed for each slice artifact then subtracted. Third, the artifact residuals are estimated using basis functions derived from performing PCA on each channel's artifact segments. The reason for splitting the artifact subtraction into two steps is that the algorithm is needed to be as adaptive as possible; the algorithm needs to adjust to sudden changes in the artifact shape (due to head movement for example). Performing PCA repeatedly on small sections of the data (to make it adaptive) would produce less than optimal basis functions. On the contrary, the moving average subtraction performed in step 2 is adaptive and removes more than 98% of the artifacts. Hence, it is opted to make the bulk of the artifact removal as adaptive as possible while maintaining the efficiency of using PCA to describe and remove the residuals. Fourth, adaptive noise cancellation (ANC) is performed [5]. ANC removes any components in the data that are correlated with a reference. By using the subtracted noise as a reference, artifact components not captured in the basis set are removed. More details about the function of the ANC filter is given later. The process encompassing all the four steps is referred to as FASTR. Fig. 1 shows a schematic of the FASTR algorithm. The schematic and the following details are for a single channel of EEG data. All the four steps are discussed below.

(1) Interpolation and Alignment of Slice-Timing Trigger

During the acquisition of simultaneous EEG/FMRI data, triggers are sent by the MRI machine at the start of each slice acquisition. These triggers are usually a simple 5-V TTL signal that can be read by the EEG amplifier and inserted in the data to indicate the starting location of each slice acquisition and the corresponding slice artifact (to be used in subsequent steps to form the artifact template). However, since the MRI machine and the EEG system are driven by separate clocks, some degree of misalignment—''jitter''—may occur in the exact location of the registered trigger relative to the artifact from one slice to the next. The jitter gets worse as the EEG sampling rate is reduced. Relying on these triggers for time-locking slices to construct an artifact template would therefore not be optimal. To remedy this problem, the first channel data (or any other EEG channel data) is sync interpolated (up-sampled) to bring the sampling rate to about 20 kHz and then divided into segments according to the slice-timing triggers [7]. In this thesis paper, the term artifact segment is used to indicate a window covering the duration of a single slice artifact occurrence. The first artifact segment is then taken as a reference. For each of the remaining slice artifact segments, the trigger location is adjusted to maximize the correlation with the reference. Although this process can be repeated for each EEG channel, this is not only computationally inefficient but is also unnecessary. It is found that in practice adjustments to one EEG channel apply equally to them all.

(2) Subtraction of Local Slice artifact Template

For any interpolated channel, $\mathbf{Y}^a$, which is collected during the acquisition of continuous FMRI, a 1-Hz high-pass filtered version, $\mathbf{Y}^h$ is generated. The high-pass filter serves to remove any slow drifts in the EEG to ensure that the different artifact segments used in the average artifact estimation have the same baseline. This is useful since the artifact signal itself is unlikely to have any slow drifts or shifts in the baseline from one segment to another, thus the high-pass filtering will improve the artifact estimation. $\mathbf{Y}^h$ is then segmented into N (N = volumes × slices) equal-sized segments according to the adjusted/aligned slice-timing triggers. Each of these segments is a 1 × q vector, where q is the number of time points spanning each artifact interval. The local moving average artifact template for each segment is calculated then as:

$$\mathbf{A}_j = \frac{1}{|I(j)|}\sum_{l\in I(j)} \mathbf{Y}_l^h \qquad (1)$$

In Eq. (1), j = 1, 2 . . . N indexes the slice artifact segments, **A***j* is a 1 × q vector of the local moving average artifact template for segment *j* and *l* is an index of the different artifact segments to be averaged [7].

I(j) is an index function, which determines which segments are included in the average. The slice segments in ***I(j)*** are centered around segment *j* and are chosen so that there is a sufficient time gap between them to ensure that there is no EEG autocorrelation between the segments included in the template computation. This approach removes any data that

correlates with the FMRI slice acquisition indiscriminately. The user needs only to determine how many elements to include in $I(j)$, i.e., the length of the moving average window, and how much gap to leave between the selected segments. The selection of averaging window length $|I(j)|$ governs the adaptivity of the algorithm to changes in the artifact waveform (due to head movement for example). The shorter the window length, the more adaptive the algorithm. On the other hand, the shorter the window length, the more noisy the artifact template and the more real EEG data are likely to be removed. The gap between selected segments should be judged by how close the segments are in time. Based on experience, it is safe to assume that on the time scale of a slice artifact, EEG is uncorrelated after 350 ms. Hence, a gap of at least that much time should be left between successive segments included in the average. Finally, the computed template, $\mathbf{A}j$, is scaled by a constant a to minimize the least squares between the template and the data. We can then subtract the scaled artifact from $\mathbf{Y}^h$ to construct a signal, $\mathbf{Y}^r$, which is the cleaned EEG data with residual artifacts.

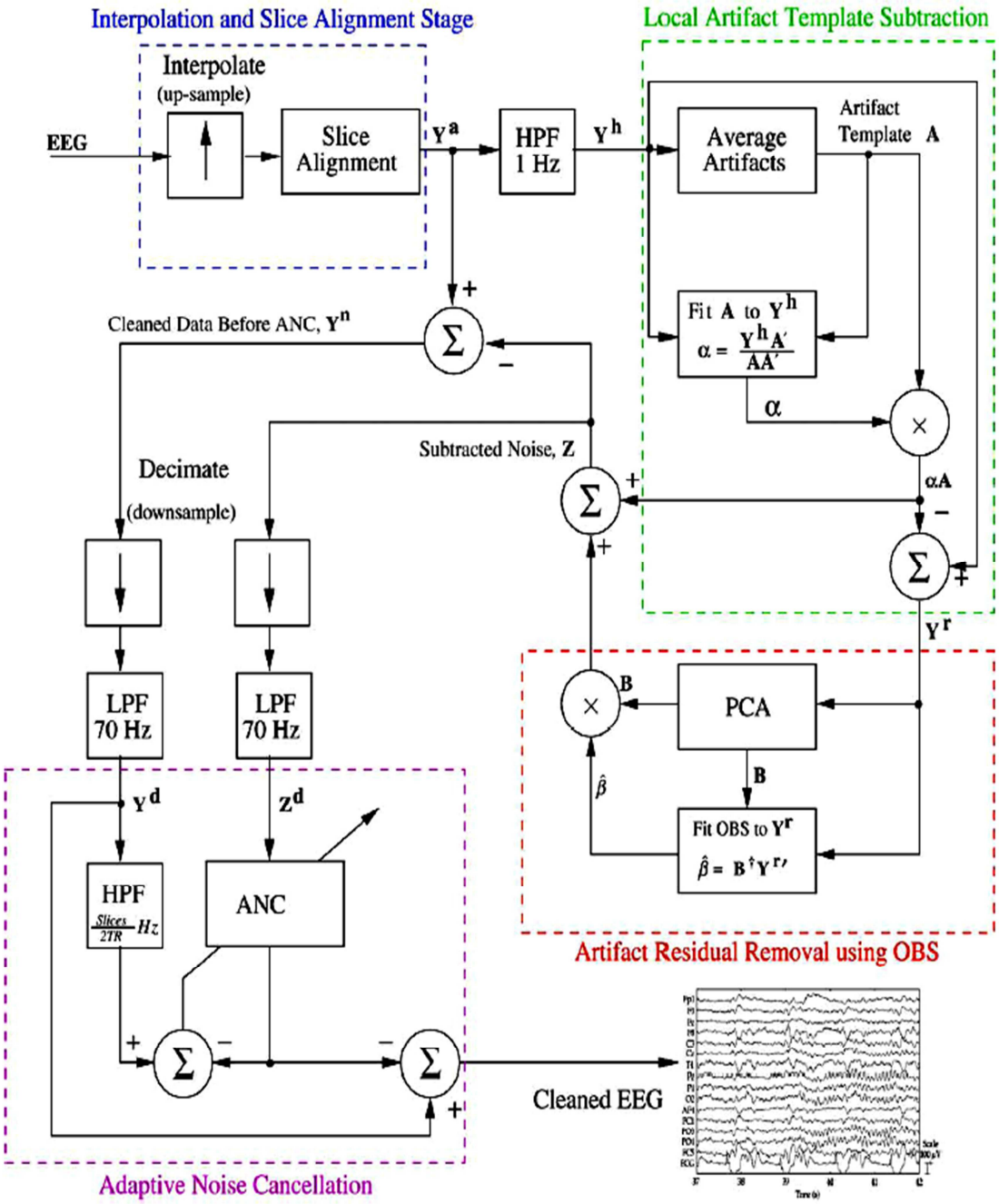

Fig.1. Schematic flow chart of the FASTR algorithm

(3) Reduction of Gradient Artifact Residual Using Optimal Basis Sets(OBS)

The vector $\mathbf{Y}^r$ that results from the previous step is still likely to be contaminated with residual artifacts due to slight variations in the shape of the artifact from one slice to the next. The amount of variation is a function of the sampling rate and the synchrony between the clocks of the MRI and EEG systems. From $\mathbf{Y}^r$, we derive a set of basis functions for the residuals. First, a residuals matrix $\mathbf{S}p \times q$ is formed, where p is the number of artifact segments included. As in the previous step, not all segments are included in **S**. Instead of a fixed gap between the selected segments, however, segments should be selected after applying a gap of s or $s + 1$ in a random order, where s is the minimum gap determined in the previous step. This is to safeguard against only capturing variations that occur every $s + 1$ segments and to insure that all variations of the artifact residuals are sampled. For example, if it were determined in step 2 that one slice artifact segment should be skipped (i.e., $s = 1$) when calculating the local artifact, then in selecting segments to include in **S**, we would sometimes skip one segment (s) and other times skip two segments ($s + 1$), in no particular order (randomly). The rows of **S** are then demeaned, i.e., the mean of each segment is removed. The column-wise mean is also calculated and subtracted from the columns of **S**, i.e., the mean effect of the residuals is calculated and removed. PCA is then performed on **S**. The different variations in the residual artifacts will be captured in the principal components of **S**, ordered according to the variance explained by each component. For simplicity, we use the term principal component (PC) to refer to the projection of **S** onto the principal component coefficients. The first C PCs, including the calculated mean effect, constitute an optimal basis set (OBS), $\mathbf{B}q \times c$for describing the gradient artifact residuals variations. The number of components C is selected based on the amount of variance explained by the PCs. It was observed that for most channels in a single data set, the same number of components is needed to explain the variance of the artifact. It is recommended that C is chosen conservatively, since including unnecessary components may result in the loss of data.

Each segment of $\mathbf{Y}^r$ can now be written in terms of **B** as:

$$\mathbf{Y}_j^{r'} = \mathbf{B}\beta_j + \varepsilon_{j'} \quad (2)$$

where β_j is a $C \times 1$ vector of weights to fit **B** to $\mathbf{Y}^r$ and ε_j is a an error term for the segment [7]. The weights for each segment are then estimated by least squares and added to the artifact noise found in step 2 to construct the final estimation of the gradient artifacts, Z, and an artifact-subtracted EEG data $\mathbf{Y}^n$ (Figure 1).

The final estimated noise is subtracted from the original interpolated EEG data, not the high-pass filtered version used for the artifact estimation, since the removed baseline drifts or slow oscillations might be of interest to the user. Both **Z** and $\mathbf{Y}^n$ are low-pass filtered at 70 Hz then down-sampled back to the original sampling frequency to form $\mathbf{Z}^d$ and $\mathbf{Y}^d$, respectively. Although steps 2 and 3 contribute to the same desired outcome, the approach taken in each is complementary to the other. In general, the process as a whole should be adaptive and accurate. Step 2 works to remove the bulk of the artifact variance and is adaptive to sudden changes in the artifact shape. However, the moving average approach in step 2 does not capture the exact artifact shape. Step 3 serves to remove the details of the residuals. This necessitates that the OBS accurately describes the variations in the residuals. To this end, the residuals matrix **S** needs to have as many entries as possible for the PCA to produce an accurate OBS; this requirement limits the adaptivity of the OBS approach. At the same time, PCA need not be performed on the whole length of the recording. In this implementation, each 1-min portion of the data is processed at a time, partly for computer memory concerns, but also to provide a degree of adaptivity.

(4) ANC (Adaptive Noise Cancellation)

The final step is the removal of any remaining residuals using adaptive noise cancellation (ANC). Figure 1 includes a schematic of the ANC filter. In ANC, a signal contaminated with noise constitutes the input to the filter, **Y**. The source of the noise is assumed to be known and is referred to as the reference signal. The actual noise in the signal is assumed to be correlated with the reference in an unknown manner. The ANC filter holds a vector of weights, which is used to calculate the output of the filter at each time point. The weights of the filter are updated at each time point using the least mean-square (LMS) algorithm. In general, the performance of the filter is controlled by the step size, μ, and the length of the weight vector, L, which control the stability and convergence of the filter. When the filter converges, it estimates the noise from the signal that is correlated with the reference. However, the accuracy of the estimation is limited by the quality of the reference and choice of μ and L. Also, high power fluctuations in the input can cause the filter to diverge [7].

In FASTR, the final artifact estimation $\mathbf{Z}^d$ is used as the reference in the ANC. Since ANC removes from the data components that are correlated with the reference, the subtracted noise Z provides a more accurate reference for this purpose and was found to have less of an effect on real data. Additionally, the input to the ANC filter is a high-pass filtered version $\mathbf{Y}^d$. The cut-off frequency is selected to be half of the fundamental gradient artifact frequency, i.e., fc = slices/2TR. The output of the filter is then subtracted from the original $\mathbf{Y}^d$ to produce the final clean EEG data.

It is found that the ANC filter consistently converged and removed components which were clearly related to the artifact. However, on its own it fails to adapt quickly enough to adequately remove all residuals. This is probably due to not providing an accurate enough reference. In addition, on its own, ANC occasionally diverges when applied to channels with high amplitude residuals. However, it is found that applying it as a last step removes any remaining residuals even though in most cases they are not detectable by visual inspection. These residuals can be due to the fact that the basis functions in the OBS do not perfectly describe all residual variations.

2.2 ALGORITHM FOR BALLISTOCARDIOGRAPHIC ARTIFACT REDUCTION

Like gradient artifact residuals, BCG artifacts are time varying. However, the variations in BCG artifacts are unpredictable and more difficult to characterize. It is assumed that each occurrence of a BCG artifact, in any given EEG channel, is independent of any previous occurrence. Moreover, it is assumed that the different occurrences are sampled from an unknown set of possible variations. These assumptions present the use of OBS as an ideal solution, where the principal variations can be captured by doing a PCA analysis on a matrix of BCG artifact occurrences [7].

- All QRS peaks are shifted forward in time by 210 ms, which is a standard delay between QRS complexes and the occurrence of BCG artifacts.
- For each channel in the EEG data, all BCG artifact occurrences are aligned in a matrix **A.** The rows of **A** are then demeaned. The column-wise mean is also calculated and subtracted from the columns of **A**, i.e., the mean effect of the residuals is calculated and removed.
- Then PCA is performed on **A**. The different variations in the artifacts will be captured in the principal components of the matrix, ordered according to the variance explained by each component. For simplicity, the term principal component (PC) is used to refer to the projection of the matrix onto the principal component coefficients.
- The first 3 PCs (including the mean effect) are taken as an OBS **B** for describing the ballistocardiographic artifacts variations. Then the EEG signal of the considered channel can be expressed in terms of **B** as:

$$X_l = \mathbf{B}\alpha_l + \varepsilon_l \quad (9)$$

Where, α_j is a 4×1 vector of weights to fit **B** to **X** and ε_l is an error term for the BCG artifact segment and *l* is is the indexes of BCG artifact segments.

- The OBS is then fitted to, and subtracted from, each BCG artifact occurrence. The process is repeated for each channel.

3 EEG DATA ANALYZING TOOLBOX

To Analyze the EEG data collected inside the MR scanner two toolboxes are used in this thesis both of which are integrated as plug-ins in EEGLAB, which is a very popular graphical toolbox for EEG analysis and visualization in MATLAB. The FMRIB (Functional Magnetic Resonance Imaging of Brain) plug-in is a set of MATLAB tools which allow the removal of FMRI-related artifacts from EEG data. These tools are designed to work within the EEGLAB environment, providing a GUI to remove FMRI gradient artifacts, detect QRS complexes from an ECG channel, and remove pulse (ballistocardiographic/BCG) artifacts from the EEG [15]. The schematic diagram of the processing steps of removing artifacts is demonstrated in Fig. 2.

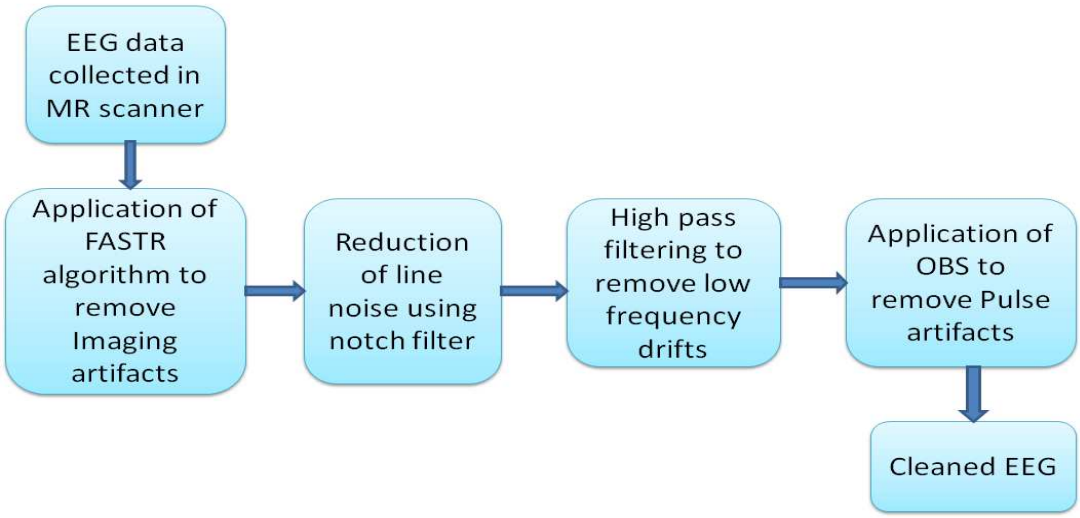

Fig.2. Processing steps of removing Gradient and Ballistocardiographic artifacts

4 EEG DATA SOURCE

The data used in this thesis is a secondary data collected during an fMRI recording session using EPI (Echo Planer Imaging) sequence [15]. The data was collected from 32 channels according to the 10-20 international system. The last two channels are EMG and ECG channels. The data (including the EMG and ECG channels) were sampled at 2048 Hz. The sampling rate of the data should be sufficient as to not have any aliasing from high frequency gradient noise (maximum gradient artifact frequency in a typical EPI sequence is about 700-800Hz). FMRI setting were TR=3s, 21 slice per volume for a total scanning time of 2mins. There were 40 FMRI volumes collected, resulting in 840 slices. The subject was instructed to open and close his eyes in periods of 10 s during scanning using the scanner communication system and earphones. The data include an event type 'slice' for each slice collected. Fig. 3 shows the original data which is contaminated with imaging or gradient artifacts, pulse or ballistocardiographic artifacts and line noise.

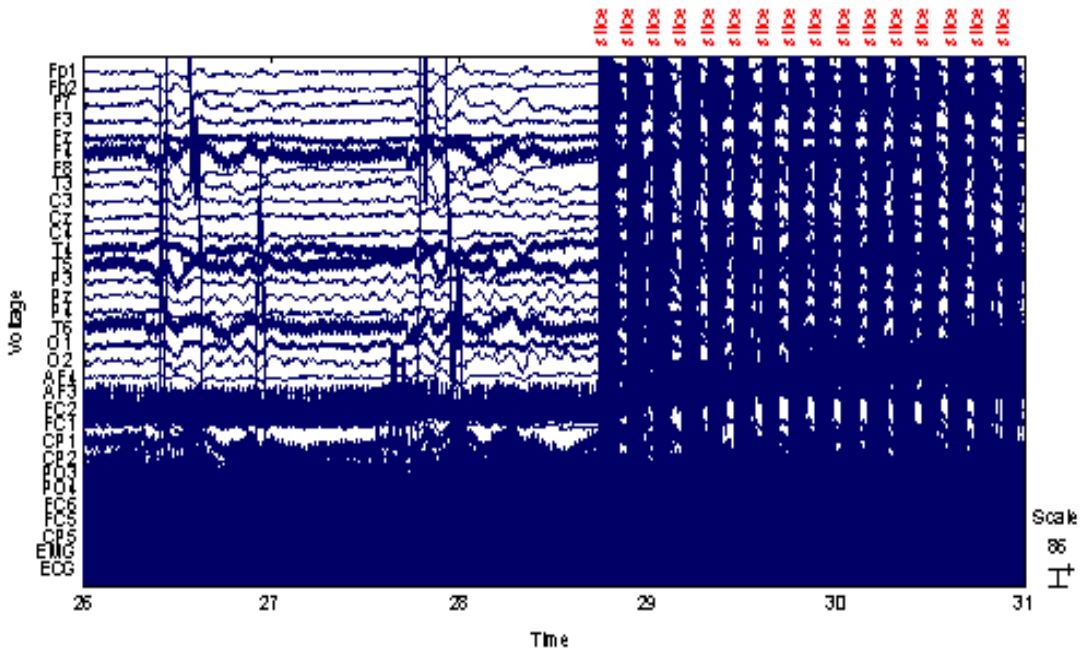

Fig. 3. EEG data frame of 2 mins containing imaging, pulse and line noise

5 RESULTS

Fig. 4 below shows the EEG data free of imaging artifact. The red lines are the slice triggers indicating the start of the FMRI acquisition. The high amplitude ECG signal can also be noticed. The pulse or BCG artifacts correlated with the ECG is also evident from the Figure. It can be noticed that using the subtracted overall noise from steps 1 to 3 as a reference in the filter instead of a binary vector was less likely to remove real data. This can be noticed in the shape of the BCG artifacts, as using the subtracted noise as a reference did not cause the shape to distort. It is evident from the Figure that imaging artifacts are entirely minimized.

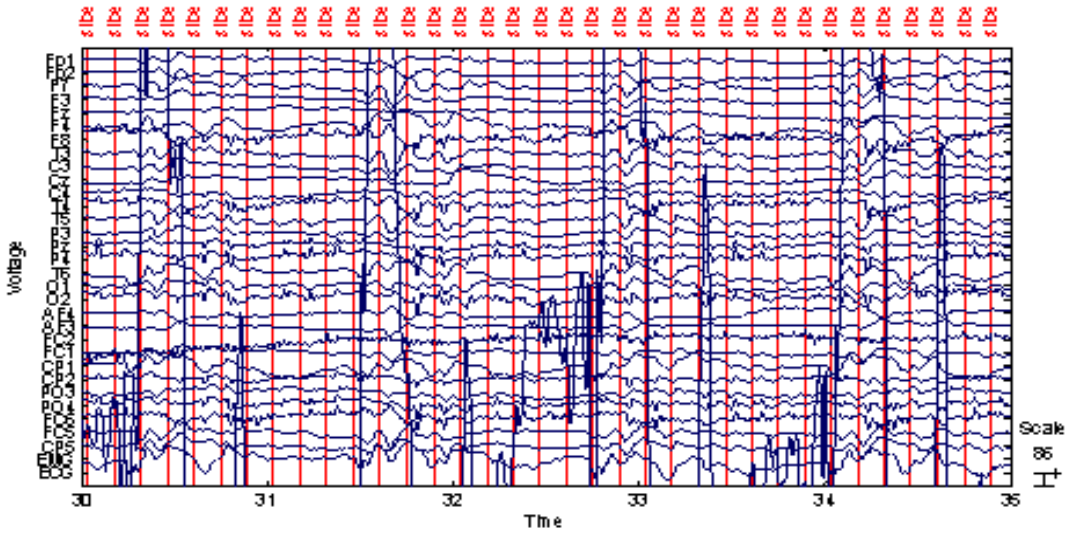

Fig. 4. EEG data after removal of gradient artifact using FASTR algorithm

Fig. 5 shows the EEG signal after the correction of pulse artifact using optimal basis sets. It is observed from the fig that about 10s after the start of FMRI (at about 39.5s) the alpha rhythms start and then disappear after another 10s. This corresponds to the opening and closing of the eyes in the experiment.

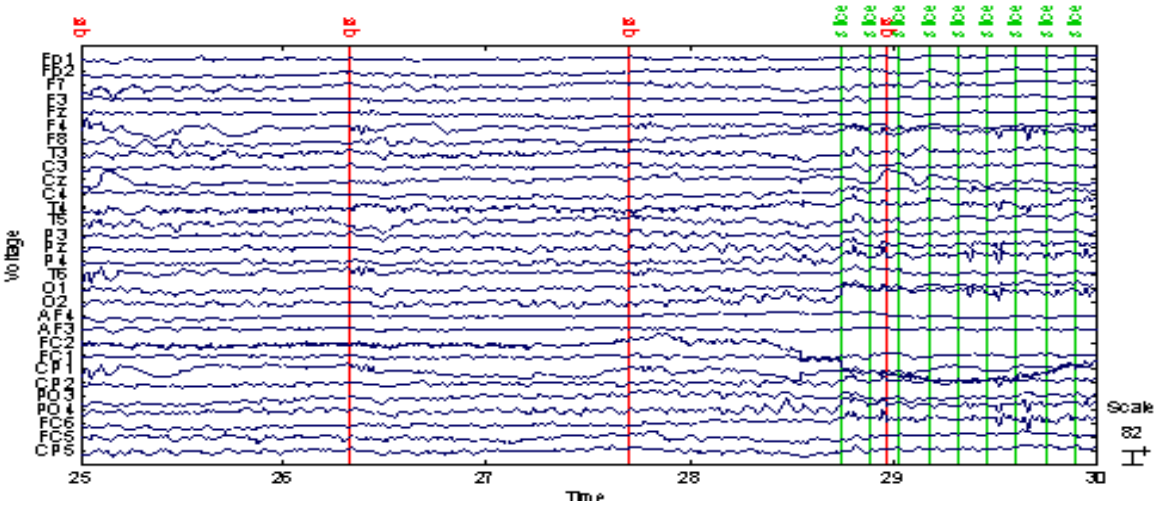

Fig. 6. Quality of EEG after correcting Ballistocardiographic artifacts using OBS

6 CONCLUSION

As was said at the start of this paper, Simultaneous EEG and FMRI is a potentially powerful technique in functional neuroimaging. Along with the potential benefits, comes a series of challenges in implementing such a technique. The main

obstacles are artifacts from MRI gradients and ballistocardiographic effects superimposed on the normal EEG, as well as the need for practical implementations of methods for their removal.

In this study, an algorithm is presented which removes gradient artifacts and any residuals from data sampled at only 2048 Hz, without the need to adjust any hardware or imaging sequences. Because of the nature of EEG data, it is difficult to assess the quality of the EEG using a simple measure. However, it is quite evident that majority of the artifacts are reduced significantly. Applying these algorithms to practical cases and troubleshooting the problems if come any will be the future focus of the work.

REFERENCES

[1] Allen, P.J., Polizzi, G., Krakow, K., Fish, D.R., Lemieux, L., 1998. Identification of EEG events in the MR scanner: the problem of pulse artifact and a method for its subtraction. NeuroImage 8 (3), 229–239.

[2] Dr. Christoph Mulert and Louis Lemieux, "EEG–fMRI: Physiological Basis, Technique and Applications", Springer.

[3] Hoffmann, A., Ja¨ger, L., Warhahn, K.J., Jaschke, M., Noachtar, S., Reiser, M., 2000. Electroencephalography during functional echo-planar imaging: detection of epileptic spikes using post-processing methods. Magn. Reson. Med. 44, 791–798.

[4] Be´nar, C., Aghakhani, Y., Wang, Y., Izenberg, A., Al-Asmi, A., Dubeau, F.,Gotman, J., 2003. Quality of EEG in simultaneous EEG–fMRI for epilepsy. Clin. Neurophysiol. 114 (3), 569– 580.

[5] Allen, P.J., Josephs, O., Turner, R., 2000. A method for removing imaging artifact from continuous EEG recorded during functional MRI. NeuroImage 12 (2), 230– 239.

[6] Salek-Haddadi, A., Friston, K.J., Lemieux, L., Fish, D.R., 2003. Studying spontaneous EEG activity with fMRI. Brain Res. Brain Res. Rev. 43 (1), 110– 133.

[7] Niazy, R. K., Beckmann, C. F., Iannetti, G. D., Brady, J. M., Smith, S. M., 2005. Removal of FMRI environment artifacts from EEG data using optimal basis sets. NeuroImage 28 (3), 720-37.

[8] Markus Ullsperger and Stefan Debener, "Simultaneous EEG and fMRI :Recording, Analysis, and Application", Oxford University press.

[9] Bonmassar, G., Purdon, P.L., Jaaskelainen, I.P., Chiappa, K., Solo, V., Brown, E.N., Belliveau, J.W., 2002. Motion and ballistocardiogram artifact removal for interleaved recording of EEG and EPs during MRI. NeuroImage 16 (4), 1127–1141.

[10] Garreffa, G., Carni, M., Gualniera, G., Ricci, G.B., Bozzao, L., De Carli, D., Morasso, P., Pantano, P., Colonnese, C., Roma, V., Maraviglia, B., 2003. Real-time MR artifacts filtering during continuous EEG/fMRI acquisition. Magn. Reson. Imaging 21 (10), 1175-1189.

[11] Anami, K., Mori, T., Tanaka, F., Kawagoe, Y., Okamoto, J., Yarita, M., Ohnishi, T., Yumoto, M., Matsuda, H., Saitoh, O., 2003. Stepping stone sampling for retrieving artifact-free electroencephalogram during functional magnetic resonance imaging. NeuroImage 19 (2 Pt. 1), 281–295.

[12] Christov, I.I., 2004. Real time electrocardiogram QRS detection using combined adaptive threshold. Biomed. Eng. Online 3 (1), 28.

[13] Mukhopadhyay, S., Ray, G.C., 1998. A new interpretation of nonlinear energy operator and its efficacy in spike detection. IEEE Trans. Biomed. Eng. 45 (2), 180– 187.

[14] Kim, K.H., Yoon, H.W., Park, H.W., 2004. Improved ballistocardiac artifact removal from the electroencephalogram recorded in fMRI. J. Neurosci. Methods 135 (1– 2), 193– 203.

[15] http://users.fmrib.ox.ac.uk/~rami/fmribplugin/#tutorial